

Legendre Expansion for Scattering Anisotropy in Analytical 1D Multigroup S_N Equations

Jilang Miao,*¹ and Miaomiao Jin*

*Department of Nuclear Engineering, The Pennsylvania State University, University Park, 16802 PA, USA

INTRODUCTION

The discrete ordinates method, commonly referred to as the S_N method [1], involves discretizing the particle transport equation in its differential form. The computation of particle fluxes relies on the direct evaluation of the transport equation at a finite set of discrete angular directions, referred to as ordinates. Additionally, quadrature relationships are employed to substitute integrals over angles, by converting them into summations over these discrete ordinates [2].

Numerous efforts in the literature have concentrated on developing one-dimensional (1D) analytical transport solutions to meet diverse needs. However, the analytic solutions are typically confined to applications characterized by spatial homogeneity, angular isotropy (or linear scattering), and one energy group [3, 4, 5, 6, 7]. Recent advancements involve the vectorization of the S_N transport equation and seeking analytical solutions through matrix inversion [8, 9]. Although these methods can handle heterogeneous 1D problems, their applicability has been limited to one-group scenarios. Furthermore, they operate as fixed source solvers, necessitating the representation of the source term using piece-wise constant functions on a fine mesh for solving eigenvalue problems [10]. Additionally, these approaches are constrained to matrices with real eigenvalues, precluding method acceleration such as redistributing more fission from the source term via Wielandt's shift [11].

To advance the capability of these methods [8, 9, 10], we previously developed an analytical solution for heterogeneous slab problems [12]. This solution, with closed-form expressions for S_2 and two energy groups, eliminates the need for power iteration to address eigenvalue problems. The matrix block-diagonalization procedures employed in this analytical approach facilitate the efficient treatment of complex eigenvalues. Subsequently, the method was expanded to tackle multigroup S_N equations in slab geometry [13]. This extension characterizes the solution within each grid through an expansion based on the eigensystem determined by neutron cross sections in the material. The expansion coefficients are determined by solving a linear system that incorporates continuity conditions at the interfaces and boundary conditions of the angular fluxes. The eigenvalues are obtained by seeking the root of the determinant of the boundary condition matrix.

Furthermore, we devised a fixed source solver for the multigroup S_N equations and applied it within the power iteration framework to handle eigenvalue problems. In the study presented in [14], power iteration was executed, assuming a piece-wise constant source on a fine mesh, while the fluxes were represented on a coarse mesh characterized by distinct materials. In a complementary work [15], a coarse mesh iteration method was developed, wherein both flux and source

terms are expanded based on the eigensystem determined by material cross sections. This method achieves accelerated computation while maintaining the same level of accuracy.

However, a common assumption in above-mentioned methods [13, 14, 15] is that the scattering matrix is in the form of $\Sigma_{s,g'n' \rightarrow gn}$, where g and g' are indices for energy groups, and n and n' are indices for discrete angles. In the case of isotropic scattering, obtaining the matrix is straightforward from the scattering cross section without dependence on n and n' . However, for anisotropic scattering, generating such cross sections is not feasible. Anisotropic scattering is typically represented using Legendre expansion [16, 17]. In this study, we incorporate scattering anisotropy into the 1D analytical multigroup S_N equations using Legendre expansions. We demonstrate its accuracy through a comparison with Monte Carlo (MC) reference on a heterogeneous slab problem derived from a typical pincell.

METHODOLOGIES

For a given number of energy groups, denoted as $g = 1, \dots, G$, and a quadrature set $\{\mu_n, \omega_n\}_{n=1, \dots, N}$, the transport equation for the angular flux $\psi_{g,n}$ is expressed in Eq 1.

$$\begin{aligned} \mu_n \frac{\partial}{\partial x} \psi_{g,n}(x) + \Sigma_{t,g} \psi_{g,n}(x) &= \sum_{n',g'} \omega_{n'} \Sigma_{s,g'n' \rightarrow gn} \psi_{g',n'}(x) \\ &+ \frac{1}{k_{eff}} \sum_{n',g'} \omega_{n'} \nu \Sigma_{f,g'n' \rightarrow gn} \psi_{g',n'}(x) \end{aligned} \quad (1)$$

Since it is not practical to generate multigroup cross sections in the form of $\Sigma_{s,g'n' \rightarrow gn}$, we rewrite the scattering term as a function of Legendre moments. The scattering rate S from group g' to g with scattering cosine μ is conventionally written as Eq. 2,

$$\begin{aligned} S_{g' \rightarrow g}(x, \mu) &= \sum_{l=0}^L \frac{2l+1}{2} \Sigma_{s,g' \rightarrow g,l} P_l(\mu) \phi_l(x) \\ &= \sum_{l=0}^L \frac{2l+1}{2} \Sigma_{s,g' \rightarrow g,l} P_l(\mu) \int d\mu' P_l(\mu') \psi_{g'}(x, \mu') \\ &= \sum_{l=0}^L \frac{2l+1}{2} \Sigma_{s,g' \rightarrow g,l} P_l(\mu) \sum_{n'} \omega_{n'} P_l(\mu_{n'}) \psi_{g',n'}(x) \end{aligned} \quad (2)$$

Here, we replace the integral in the definition of $\phi_l(x)$ with the sum over S_N quadrature sets. With $\mu = \mu_n$ in Eq. 2 and plugging into Eq 1, we can organize the cross-sections and quadrature sets into matrices [13], and hence Eq 1 can be written in matrix form as,

$$\partial_x \Psi(x) = A \Psi(x) \quad (3)$$

where

$$A = \frac{F}{k_{eff}} + S - T \quad (4)$$

Herein, F , S , and T are the respective fission, scattering, and total cross sections multiplied by S_N quadrature set parameters $\{\mu_n, \omega_n\}_{n=1, \dots, N}$. Specifically, for scattering, we have

$$S_{gN+n,g'N+n'} = \frac{\omega_{n'}}{\mu_n} \sum_{l=0}^L \frac{2l+1}{2} P_l(\mu_n) \Sigma_{s,g' \rightarrow g,l} P_l(\mu_{n'}) \quad (5)$$

¹Corresponding author: Jilang Miao (jlmiao@psu.edu)

With this formulation, we can treat scattering anisotropy to arbitrary Legendre order. Then the multigroup S_N eigenvalue problems in heterogeneous slab systems can be solved via either the non-iterative determinant root solver [13] or the iterative methods [14, 15].

RESULTS

In this section, we test the method on a heterogeneous slab system where multigroup cross sections are generated from a pincell. Results including k_{eff} , scalar fluxes and angular fluxes from S_4 , S_8 , S_{16} , and S_{32} will be compared with a MC reference.

Description of the test case

We consider a pincell with UO_2 fuel, helium gap, zircaloy cladding and borated water. The pincell has a pitch of 1.323 cm and length of 30 cm. Two borated water regions with 2.5 cm thickness are on the ends of the fuel, respectively. Boundary conditions are vacuum axially and reflective radially. Two-group cross-sections are generated with OpenMC [18, 19] with scattering Legendre moments of order 4 (P_4). The pincell is homogenized to a slab problem with the core of length 30cm and two reflector regions of length 2.5cm on both ends. The cross sections for the core and reflector materials are shown in Table I.

TABLE I. Cross-section parameters.

	Core	Reflector
$\Sigma_{t,1}$	6.8294e-01	8.9176e-01
$\Sigma_{t,2}$	2.0658e+00	3.0361e+00
$\Sigma_{s,0,1\rightarrow 1}$	6.4870e-01	8.4530e-01
$\Sigma_{s,0,1\rightarrow 2}$	2.5869e-02	4.6078e-02
$\Sigma_{s,0,2\rightarrow 1}$	4.2114e-04	2.8498e-04
$\Sigma_{s,0,2\rightarrow 2}$	1.9696e+00	3.0181e+00
$\Sigma_{s,1,1\rightarrow 1}$	3.2525e-01	5.0694e-01
$\Sigma_{s,1,1\rightarrow 2}$	7.7637e-03	1.4061e-02
$\Sigma_{s,1,2\rightarrow 1}$	2.2069e-04	2.0111e-04
$\Sigma_{s,1,2\rightarrow 2}$	4.4646e-01	6.6720e-01
$\Sigma_{s,2,1\rightarrow 1}$	1.3329e-01	2.0454e-01
$\Sigma_{s,2,1\rightarrow 2}$	-2.5799e-03	-4.6366e-03
$\Sigma_{s,2,2\rightarrow 1}$	1.3804e-04	1.2919e-04
$\Sigma_{s,2,2\rightarrow 2}$	9.3323e-02	1.2844e-01
$\Sigma_{s,3,1\rightarrow 1}$	1.1392e-02	1.2657e-02
$\Sigma_{s,3,1\rightarrow 2}$	-3.0492e-03	-5.4962e-03
$\Sigma_{s,3,2\rightarrow 1}$	7.1796e-05	6.7691e-05
$\Sigma_{s,3,2\rightarrow 2}$	2.1589e-02	2.8195e-02
$\Sigma_{s,4,1\rightarrow 1}$	-1.4437e-02	-2.8207e-02
$\Sigma_{s,4,1\rightarrow 2}$	-6.6600e-04	-1.1974e-03
$\Sigma_{s,4,2\rightarrow 1}$	2.2672e-05	2.2173e-05
$\Sigma_{s,4,2\rightarrow 2}$	-2.7343e-03	-5.7950e-03
$\nu\Sigma_{f,1}$	6.0427e-03	0.0000e+00
$\nu\Sigma_{f,2}$	1.5343e-01	0.0000e+00
χ_1	1.0000e+00	0.0000e+00
χ_2	0.0000e+00	0.0000e+00

Scattering anisotropy

In addition to obtaining the multigroup cross sections, the continuous energy Monte Carlo simulation on the original pincell yields its eigenvalue at $1.13604 \pm 2\text{pcm}$. Subsequently, we perform a multigroup MC simulation to generate a reference for the slab problem, utilizing the cross-sections as listed in Table I. The eigenvalue of the slab is determined to be 1.16055

$\pm 1\text{pcm}$. Assuming isotropic scattering and neglecting the higher Legendre moments, the eigenvalue of the slab is calculated to be $1.24953 \pm 2\text{pcm}$. The k_{eff} values are summarized in Table II. Within the total 11349 pcm error of the isotropic model, the discrepancy between isotropic and P_4 scattering accounts for 8895 pcm k_{eff} error, while the remaining 2454 pcm error is attributed to radial homogenization, the two-group approximation, and higher-order scattering moments.

TABLE II. k_{eff} reference of different models.

Energy	Model Configuration Scatter	Geometry	k_{eff}	diff (pcm)
	ENDF/B-VII.1	3D	$1.13604 \pm 2\text{pcm}$	
2 group	isotropic	slab	$1.24953 \pm 2\text{pcm}$	-11349
2 group	P_4	slab	$1.16055 \pm 1\text{pcm}$	-2454

Scattering anisotropy is also demonstrated by the scattering angle distribution for each incoming and outgoing energy group in core and reflector. The scattering angle distribution from both MC tallies and Legendre expansions are given in Fig. 1. Here, the scattering distributions are calculated using Eq. 6 with cross sections from Table I. The consistency between MC tallies and Legendre expansion demonstrates that P_4 is accurate enough to capture the anisotropy of the problem. In particular, the probability density function of the scattering angle clearly shows the scattering is not isotropic.

$$\sum_{l=0}^4 P_l(\mu) \Sigma_{s,g' \rightarrow g,l} \quad (6)$$

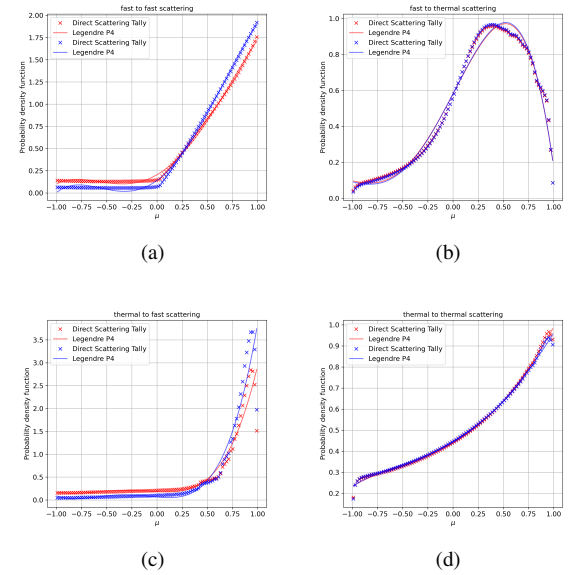


Fig. 1. Scattering Angle distribution. The crosses are based on tallies from the continuous MC simulation, and the solid curves are from P_4 Legendre expansion.

Numerical Results

The reference for the test case is derived using the multigroup mode of OpenMC. The simulation tracks 2×10^6 neutrons per generation. Neutrons are simulated for 200 inactive generations, and tallies are collected for the subsequent 1000

active generations to compute scalar fluxes, angular fluxes, and k_{eff} . Fluxes are tallied on a spatially uniform mesh with a size of 700 for each energy group. Additionally, angular fluxes are tallied over a specific polar angle range corresponding to the S_N quadrature set.

We then solve the eigenvalue of the heterogeneous slab with the analytical multigroup S_N methods introduced in [13, 14, 15]. All the methods return the eigenvalue and expansion coefficients for angular fluxes. The expansion coefficients are then used to evaluate the angular fluxes on the same 700 spatial mesh to compare spatially-dependent flux values. The results from these methods on S_4, S_8, S_{16}, S_{32} are compared in Table III. The ‘‘Determinant Root Solver’’ method builds the linear system from boundary conditions and interface angular flux continuity conditions on the coarse mesh [13]. It determines the eigenvalue as the root of the determinant of the boundary condition matrix and solves the angular flux coefficients as the null space of the boundary condition matrix. The ‘‘Coarse Mesh Iteration’’ method represents both angular flux and source term on the coarse mesh and updates the coefficients via power iteration [15]. The ‘‘Fine Mesh Iteration’’ method represents the source term as piece-wise function on the fine mesh, solves the angular flux expansion coefficients on the coarse mesh and updates the coefficients via power iteration [14]. The values under ‘mesh’ column correspond to the grid number in each region with a format (reflector-core-reflector); for the fine mesh method, there is a fourth number which is the grid size for the source term.

Table III distinctly illustrates the convergence of the solution toward the Monte Carlo reference, reducing from -48 pcm for S_4 to less than 1 pcm for S_{32} . Additionally, it is noteworthy that all the analytical methods evaluated exhibit eigenvalue differences below 0.1 pcm.

TABLE III. k_{eff} from S_N compared with MC reference.

Method	k_{eff}	error (pcm)
MC reference	$1.160548 \pm 1.5\text{pcm}$	
Determinant Root Solver		
order	mesh	
S_4	(1-4-1)	-47.9
S_8	(1-9-1)	-9.3
S_{16}	(2-18-2)	-1.4
S_{32}	(3-30-3)	0.4
Coarse Mesh Iteration		
order	mesh	
S_4	(1-4-1)	-47.9
S_8	(1-9-1)	-9.3
S_{16}	(2-18-2)	-1.4
S_{32}	(2-36-2)	0.4
Fine Mesh Iteration		
order	mesh	
S_4	(1-4-1+696)	-47.9
S_8	(1-9-1+693)	-9.3
S_{16}	(2-18-2+686)	-1.4
S_{32}	(2-36-2+680)	0.4

Next, we proceed to compare the scalar fluxes, as illustrated in Fig. 2, which includes results from S_4, S_8, S_{16} and S_{32} . For each order, the scalar fluxes from S_N and MC are compared for fast and thermal groups, respectively. Within each subfigure, the upper plots show the accurate match of the scalar fluxes, while the bottom plots depict the point-wise

relative error in percentage between S_N and MC references. Notably, as the orders increase, a significant improvement in performance is observed. The point-wise relative error decreases from around 3% in S_4 to around 0.1% in S_{32} , bringing it within the range of MC result uncertainties.

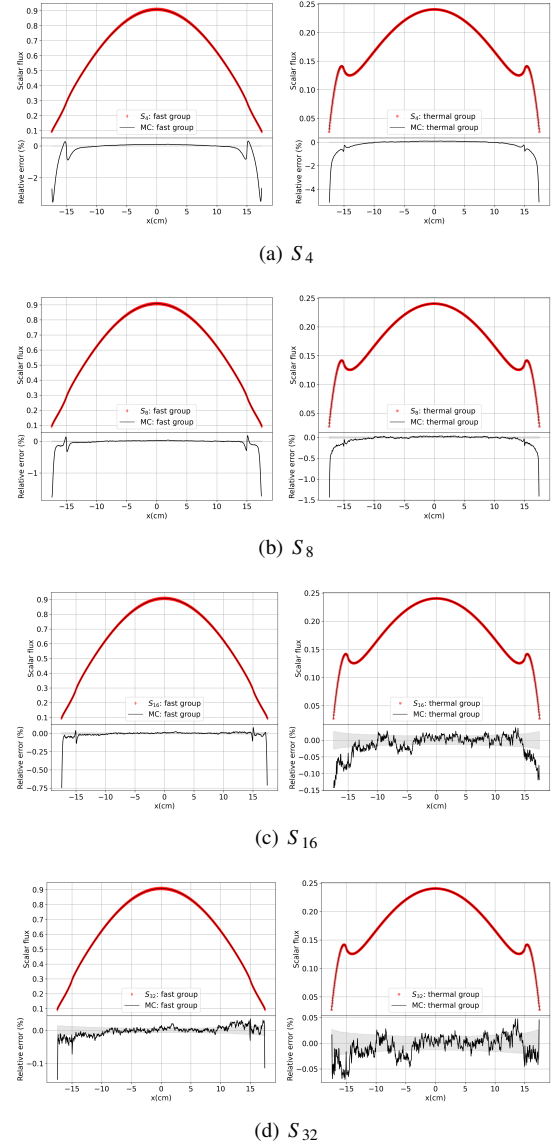


Fig. 2. S_N scalar fluxes compared with MC. For each figure, the upper part plots MC reference in solid curve and S_N results with diamond symbol for fast group and circle symbol for thermal group, and the lower part plots the pointwise relative error (%) between S_N and MC. The standard deviation of each tally T from MC is shown with the shading area between $\pm 100 \times \frac{\sigma_T}{T}$.

We observe similar patterns in the angular fluxes. In Fig. 3, we present the maximum relative error among the discrete angles for each energy group and spatial position. Due to the discretization error with too few angles, we observe a maximum relative error of around 25% for S_4 and 8% for S_8 , respectively. The maximum relative error decreases to around 1% for S_{32} . Additionally, we note that for S_4 and S_8 , where the k_{eff} error is over -9pcm (see Table III), the maximum error is biased in the negative range. Conversely, when the k_{eff}

error decreases to below 1pcm, the maximum error becomes symmetric about 0. The errors are more prominent at the slab boundaries due to the reference values being close to 0, influenced by vacuum boundary conditions.

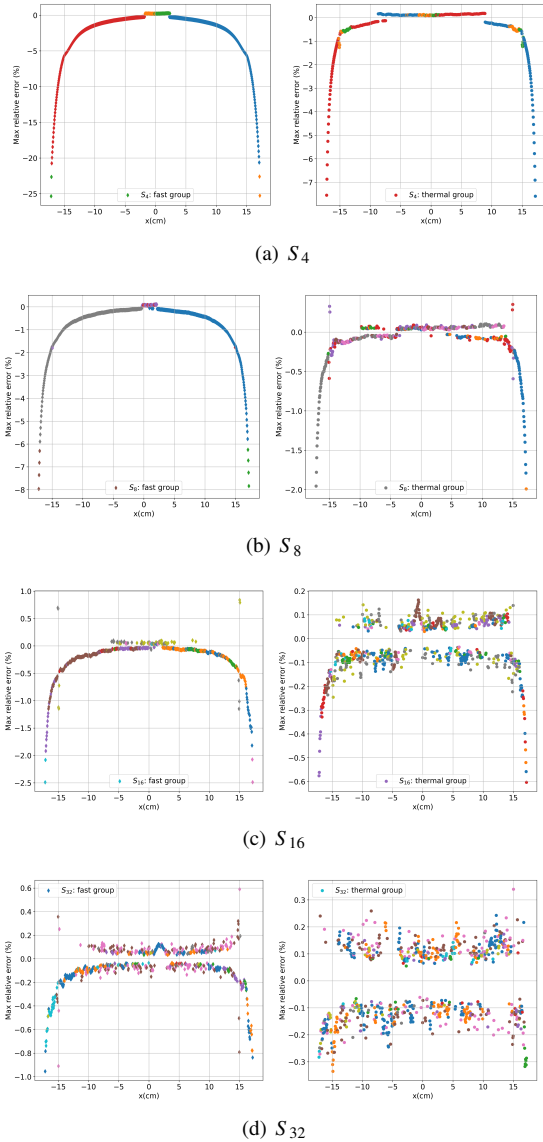


Fig. 3. S_N angular fluxes compared with MC. The values plotted are the maximum relative error (%) of angular flux for each group and each location. The scatter colors are coded by the angles where the maximum error occurs.

CONCLUSIONS

In this study, we showcased the treatment of scattering anisotropy using the analytical methods developed in our previous work for solving multigroup S_N equations in slab geometry. For the slab problem derived from a typical pincell, we achieved -47.9pcm eigenvalue accuracy for the S_4 solution and less than 1pcm eigenvalue accuracy in the S_{32} solution. Notably, high accuracy was also observed in angular fluxes. As part of future work, we plan to extend the 1D solver to 3D neutron transport using schemes such as $2D - 1D$ coupling

and 3D nodal methods.

ACKNOWLEDGMENTS

This work is supported by the Department of Nuclear Engineering, The Pennsylvania State University.

REFERENCES

1. B. G. CARLSON, "Solution of the Transport Equation by S_N Approximations," Tech. Rep. LA-1599, Los Alamos Scientific Laboratory (1953).
2. A. HÉBERT, *Applied Reactor Physics*, Presses inter Polytechnique (2009).
3. C. SIEWERT and P. ZWEIFEL, "AN EXACT SOLUTION OF THE EQUATIONS OF RADIATIVE TRANSFER," *Trans. Amer. Nucl. Soc.*, **8** (1965).
4. R. C. DE BARROS and E. W. LARSEN, "A numerical method for one-group slab-geometry discrete ordinates problems with no spatial truncation error," *Nuclear Science and Engineering*, **104**, 3, 199–208 (1990).
5. C. F. SEGATTO, M. VILHENA, and J. D. BRANCHER, "The one-dimensional LTSN formulation for high degree of anisotropy," *Journal of Quantitative Spectroscopy and Radiative Transfer*, **61**, 1, 39–43 (1999).
6. B. D. GANAPOL, "The response matrix discrete ordinates solution to the 1D radiative transfer equation," *Journal of Quantitative Spectroscopy and Radiative Transfer*, **154**, 72–90 (2015).
7. J. WARSA, "Analytical S_N solutions in heterogeneous slabs using symbolic algebra computer programs," *Annals of Nuclear Energy*, **29**, 7, 851–874 (2002).
8. D. WANG and T. BYAMBAAKHUU, "A New Analytical S_N Solution in Slab Geometry," *Transactions of the American Nuclear Society*, **117** (2017).
9. A. ENGLISH and Z. WU, "A Semi-Analytical Solution to the 1D S_N Transport Equation for a Multi-Region Problem," in "ANS Student Conference," Virginia Commonwealth University, Richmond, VA (Apr 4-6 2019).
10. D. WANG, "Solving Neutron Transport K-Eigenvalue Problems Using the ANDO Method," *Transactions of the American Nuclear Society*, **126**, 268–271 (2022).
11. F. BROWN ET AL., "Wielandt acceleration for MCNP5 Monte Carlo eigenvalue calculations," in "Joint International Topical Meeting on Mathematics & Computation and Supercomputing in Nuclear Applications (M&C+SNA 2007), Monterey, California," (2007).
12. J. MIAO and M. JIN, "An Analytic Method for Solving Static Two-group, 1D Neutron Transport Equations," *Transactions of the American Nuclear Society*, **127**, 1068–1071 (2022).
13. J. MIAO and M. JIN, "An Accurate S_N Method for Solving Static Multigroup Neutron Transport Equations in Slab Geometry," *Transactions of the American Nuclear Society*, **129**, 926–929 (2023).
14. J. MIAO and M. JIN, "Developing an Analytical Fixed Source Solver for the 1D Multigroup S_N Equations," *arXiv:2401.15763* (2024).
15. J. MIAO and M. JIN, "Coarse Mesh Iteration Approach for Analytical 1D Multigroup S_N Eigenvalue Problems," *arXiv:2401.15765* (2024).
16. W. M. STACEY, *Nuclear Reactor Physics*, John Wiley & Sons (2018).
17. Y. WANG, S. SCHUNERT, J. ORTENS, V. LABOURE, M. DEHART, Z. PRINCE, F. KONG, J. HARTER, P. BALESTRA, and F. GLEICHER, "Rattlesnake: A MOOSE-based multiphysics multischeme radiation transport application," *Nuclear Technology*, **207**, 7, 1047–1072 (2021).
18. P. K. ROMANO and B. FORGET, "The OpenMC monte carlo particle transport code," *Annals of Nuclear Energy*, **51**, 274–281 (2013).
19. W. BOYD, A. NELSON, P. K. ROMANO, S. SHANER, B. FORGET, and K. SMITH, "Multigroup cross-section generation with the OpenMC Monte Carlo particle transport code," *Nuclear Technology*, **205**, 7, 928–944 (2019).